

Clogging in bidisperse granular flow: a parametric study

Sukhada C. Bhure^{1,2} and Ashish V. Orpe^{1,2,*}

¹CSIR-National Chemical Laboratory, Pune 411008 India

²Academy of Scientific and Innovative Research (AcSIR), Ghaziabad 201002 India

Abstract. We have investigated the clogging behavior of aspherical particles flowing in a silo in the presence of a small amount of spherical particles. The primary focus of the work is to study the effects of particle shape and size of secondary spheres, using Discrete Element Method (DEM) simulations. We observe that the tendency of clogging increases for a small amount of secondary spheres but subsides at higher sphere content. This non-monotonic dependence is reasoned out to be due to competing effects of local packing and reduced effective particle size at the exit observed while moving from low to high sphere volume fraction. The sensitivity of clogging to local packing of particles is also evident from the observed non-monotonic dependence on the size ratio and as well the dependence of clogging on aspect ratio of bulk particles. Overall, the clogging behavior is observed to be governed by the interplay between particle alignment and packing structure, which determines avalanche strength and arch formation.

1 Introduction

Granular clogging, caused by the spontaneous formation of stable arches, is a critical issue in industrial systems wherein the particles flow through confined geometries. This phenomenon significantly impacts processes in various industries such as pharmaceuticals, food processing, and construction, where bulk materials are transported through hoppers and silos. Interestingly, the clogging-unclogging phenomena have also been extended to natural systems like movement of pedestrians or animals through a narrow exit [1, 2] or artificial systems like the flow of colloidal particles through an orifice [3]. Understanding the fundamental mechanisms governing the clogging behavior is essential for optimizing flow efficacy and preventing operational inefficiencies. While various mitigation strategies, such as vibrations, air jets, and silo modifications, have been explored [4–7], another approach involves modifying clogging behavior through bidisperse granular flows, where small secondary particles alter flow dynamics. Studies in 2D vibrated silos have shown that adding small spheres at high volume fractions ($\phi = 0.2 - 0.4$) disrupts arch formation, reducing clogging [8, 9]. In the present work, we have studied the flow and clogging behavior of aspherical shaped particles in a flat bottomed silo in the presence of small amounts of spherical particles. The overall behavior is measured in terms of avalanche size. The clogging behavior is ascertained in terms of the variation of avalanche size with respect to different particle and system level parameters. By systematically investigating these factors, this work aims to improve the understanding of bidisperse granular clogging and flow dynamics.

*e-mail: av.orpe@ncl.res.in

2 Simulation Methodology

The discrete element method (DEM) simulations were performed, using open source LIGGGHTS software, in a flat bottom silo of height $65d_b$, width $30d_b$ and thickness $10d_b$. The dimensions were chosen so as to ensure balance between computational efficiency and realistic flow conditions. Here, d_b represents the size of the primary (or bulk) aspherical particle calculated as the diameter of an equivalent sphere volume. The parameters varied in this study were the secondary sphere fraction (ϕ), primary-to-secondary particle size ratio ($r = d_b/d_s$), where d_s is the diameter of secondary, small sized spheres and shape of the primary particle in terms of the aspect ratio (Ar) defined in later sections.

The simulation employs Hertzian contact model for calculation of force between two contacting particles. The contact force comprises of normal (F_n) and tangential (F_t) components, each of which includes two terms given as

$$\mathbf{F}_n = (k_n \delta \mathbf{n} - \gamma_n \mathbf{v}_n) \quad (1)$$

$$\mathbf{F}_t = -(k_t \Delta \mathbf{s}_t + \gamma_t \mathbf{v}_t) \quad (2)$$

where, \mathbf{n} is the unit vector along the line connecting centers of two particles, \mathbf{v}_t and \mathbf{v}_n are, respectively, the tangential and normal components of particle velocities. Both the normal elastic constant (k_n) and the tangential elastic constant (k_t) are chosen to be of the order of $10^7 \text{ mg}/d_\alpha$. The values of the normal damping term (γ_n) and tangential damping term (γ_t) are chosen to be of the order of $10^2 \sqrt{g/d_\alpha}$. The damping coefficients (γ_n) and (γ_t) inherently account for particle mass, as they are evaluated based on the standard Hertzian contact model implemented in LIGGGHTS. Here, d_α represents either d_b for bulk particles or d_s for spherical particles and g represents gravity

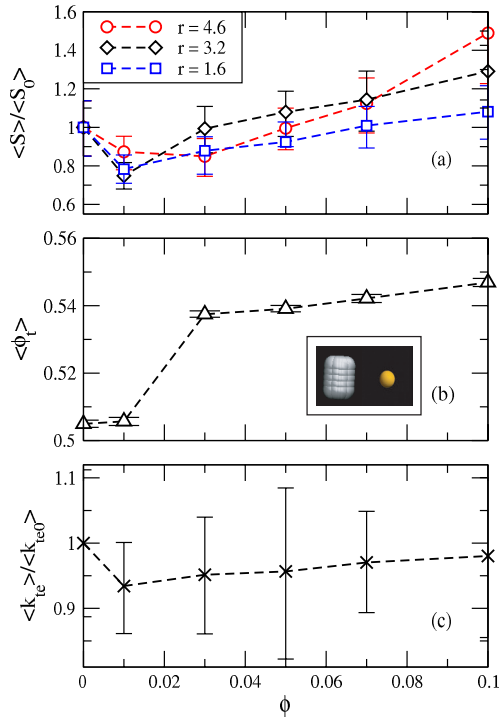


Figure 1. (a) Variation of normalized mean avalanche size ($\langle S \rangle / \langle S_0 \rangle$) with spherical particle volume fraction (ϕ). Data shown for three different particle size ratios (r). $\langle S_0 \rangle$ represents average avalanche size in the absence of spherical particles. (b) Variation of total (spheres and cylinders) average volume fraction ($\langle \phi_t \rangle$) for $r = 3.2$ (c) Variation of normalized average avalanche size ($\langle S \rangle / \langle S_0 \rangle$) with spherical particle volume fraction (ϕ) for $r = 3.2$. Error bars represent confidence interval of 95%. Inset in (b): Images showing the primary cylindrical and secondary spherical.

acting in downward direction. The values Δs_t is the tangential displacement between two particles to satisfy the Coulomb yield criterion given by $F_t = \mu_s F_n$, where μ_s is the coefficient of static friction coefficient. The integration time step used in the simulation is 10^{-4} . More details about the simulation parameters can be obtained in earlier work [10]. The clogging tendencies for different cases were evaluated by measuring the avalanche sizes. For these measurements, flow was initiated by opening the exit slit, and avalanche size was recorded as the total mass or number of discharged particles before the occurrence of clogging. Upon clogging, the flow was restarted by removing particles near the exit. This process was repeated several times to obtain statistically significant data.

3 Results and Discussion

In the following sections, we discuss the flow and clogging behavior in terms of the avalanche size and its dependence on different particle level parameters. As mentioned earlier, the avalanche size represents the amount of material flowing out of silo till the orifice is clogged. The magnitude of the avalanche size is governed by the ability of the flowing particles to form a stable arch. The increased

avalanche size represents longer flow duration before clogging takes place indicating a lesser tendency to form a stable arch and vice-versa for decreased avalanche sizes. In the limit of infinite avalanche size (flow never stops), the tendency of arch formation will be negligible and in the limit of no flow or immediate clogging, the tendency will be quite high.

3.1 Variation of secondary sphere fraction

In this and the next section, we study the effect of presence of spherical spheres on the clogging tendency of cylindrical shaped particles. The cylindrical particle, with elliptical cross-section, is shown in the inset of fig. 1b and with aspect ratio (Ar) defined as the ratio of the cylinder length to the major axis of the elliptical shaped cylinder end. The cylindrical shape is obtained using multi-sphere approach, maintaining 50 sub-spheres per particles. The variation of normalised, mean avalanche size ($\langle S \rangle / \langle S_0 \rangle$) of the mixture of cylindrical and spherical shaped particles with sphere volume fraction (ϕ) is shown in fig. 1a for three different particle size ratios (r). Here, S_0 represents the base case scenario, i.e. the avalanche size in the absence of secondary spheres. The presence of small spherical particles reduces the avalanche size compared to the base case, essentially aiding the clogging behavior. The decrease in the avalanche size is, however, observed over a limited range of sphere volume fraction, leading to a minimum in the avalanche size at an intermediate sphere volume fraction. Any further addition of spherical particles increases the avalanche size, i.e. inhibits clogging tendency. For large enough spherical particle content (ϕ) the avalanche size increases significantly. This behavior was found to be consistent with earlier studies [8, 9]. The content of spherical particles in the material exiting the silo progressively increases with increased value of ϕ , thereby lowering its mean size with respect to the orifice. This reduces the possibility of formation of stable arches, thereby leading to progressive increase in avalanche sizes. Indeed, the avalanche size will diverge at large enough spherical particle concentration approaching $\phi = 1.0$, wherein there will be primarily spherical particles in the outflow thereby precluding arch formation and hence no clog formation.

The decrease in the avalanche size is observed to coincide with a rapid increase in the total volume fraction (fig. 1b) shown for $r = 3.2$ within the region in the vicinity of the exit orifice accompanied by reduced kinetic energy (fig. 1c) shown for $r = 3.2$. We believe that the rapid increase in total volume fraction is due to spherical particles filling in the voids between aspherical particles. The combination of these two things effect results in increased tendency of arch formation leading to lower avalanche size. For large enough particle fraction, with all the voids between nearly filled, the total volume fraction now increases quite gradually (fig. 1b). However, given the increased number of smaller spherical particles exiting the silo, the average size of particles exiting the silo reduces resulting in reduced tendency to form arches, increased kinetic energy (fig. 1c) resulting in reduced tendency of arch formation and clogging, hence increased avalanche size. The

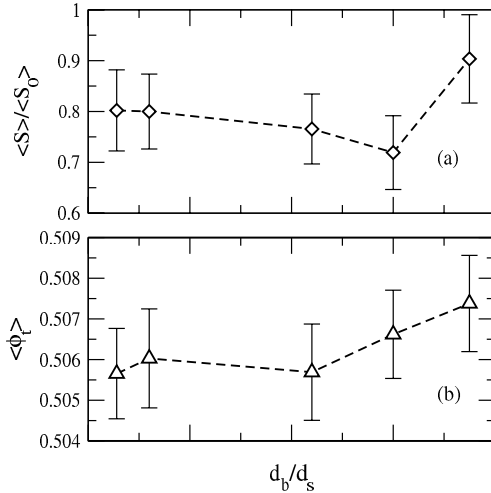


Figure 2. (a) Variation of normalized, mean avalanche size ($\langle S \rangle / \langle S_0 \rangle$) with size ratio between cylinder and sphere ($r = d_b/d_s$). (b) Variation of total (spheres and cylinders) average volume fraction ($\langle \phi \rangle$). Error bars represent confidence interval of 95%.

overall observed behavior, then, arises due to competing effects of increasing local packing fraction and reducing effective size of particles exiting the orifice with increased secondary particle fraction. We have shown the data for packing fraction and kinetic energy only for one size ratio to avoid the clutter and ease in visualization of the profiles. However, it is to be noted that similar qualitative variation is also observed for $r = 1.6$ and $r = 4.6$ suggesting consistency of the observed behavior. A more detailed analysis inclusive of the comparison to experimental observations is available elsewhere [10].

3.2 Variation of cylindrical to spherical size ratio

As mentioned in the previous section, the arch forming tendency increases at lower sphere fraction due to tendency of spheres to fill in the voids formed by bulk, cylindrical shaped particles. To investigate this further, we varied the size of the secondary spherical shaped particle while maintaining the same cylinder size as mentioned in previous section, thereby altering the size ratio (r). The sphere fraction is maintained constant at 0.01. The variation of avalanche size with the size ratio ($r = d_b/d_s$) is shown in fig. 2a. A non-monotonic dependence is seen in this case too. Since the larger (cylindrical) particle is the same, the void volume remains the same. Given that the secondary particle fraction is kept constant, the increase in size ratio represents progressive decrease in secondary (spherical) particle size. The decrease in the sphere size will correspond to more number of spheres which are expected to pack better in the same void volume leading to a monotonic increase in total volume fractions as shown in fig. 2b. This progressive increase in volume fraction results in progressively increased tendency of arch formation and reduced avalanche size. However, for small enough sphere size ($d_b/d_s = 4.57$), the avalanche size, instead, increases. We conjecture that for very small sphere sizes,

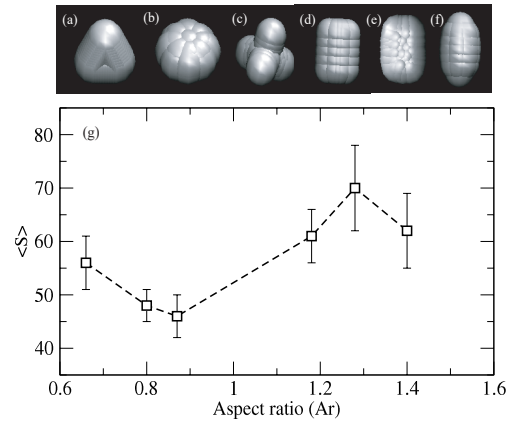


Figure 3. (a-f) Primary particles of different shapes with increasing order of aspect ratio values from left to right. (a) Tetrahedron (Ar = 0.65) (b) Oblate (Ar = 0.8) (c) Tetrapod (Ar = 0.88) (d) Cylindrical (Ar = 1.2) (e) Rectangular flake (Ar = 1.3) (f) Prolate (Ar = 1.4). (g) Variation of mean avalanche size ($\langle S \rangle$) with bulk particle aspect ratio (Ar) for fixed sphere volume fraction, $\phi = 0.01$ and size ratio, $r = d_b/d_s$. Error bars represent confidence interval of 95%.

the average particle size exiting the silo also simultaneously reduces compared to orifice size, which will reduce the tendency to form arches, hence reduced clogging and larger avalanche size. Note that this effect due to particle average size exists at all size ratios, though it starts to dominate beyond a threshold size ratio ($d_b/d_s = 4.0$), thereby resulting in reduced clogging. The underlying physics for observations discussed in secs. 3.1 and 3.2 and presented in figs. 1 and 2, then, remains the same. The reduced average size of the particles exiting the silo in both cases is due to increased number of smaller particles, though in one case it is due to increased sphere volume fraction for a fixed sphere size and in other case it is due to decreased sphere size at a fixed sphere volume fraction.

3.3 Variation in particle shape

Considering the substantial influence of local packing within the void formation on clogging tendency as observed in previous sections, the obvious parameter to study would be the particle shape, as it is expected to influence void formations substantially. We have considered six different particle shapes in this work as shown in the top panel of fig. 3. The particles shapes have been characterised in the form of aspect ratio (Ar). The aspect ratio (Ar) is defined based on the characteristic dimensions of each shape. For oblate particle, it is given by the ratio of the semi-minor axis to the semi-major axis. For a tetrapod particle, it is defined as the ratio of the longest arm length to the core diameter. In case of tetrahedral particle, this ratio is computed as the shortest edge to the longest edge. For a cylindrical particle with an elliptical cross-section (defined in sec. 3.1) and rectangular flakes, Ar is evaluated as the ratio of length to the major axis of cylinder end shape. Lastly, for prolate particle, it is determined as

the semi-major axis to the semi-minor axis. Primary particles, with different aspect ratios as shown in fig. 3, were considered to ascertain the effect of particle shape. All these particles were modeled using multi-sphere approach, maintaining 50 sub-spheres per particle. The equivalent volume diameter and mass of all the particles was kept identical across different particle shapes.

The variation of mean avalanche size ($\langle S \rangle$) with aspect ratio (r) is shown in fig. 3g. The secondary sphere fraction and the size ratio was maintained constant at 0.01 while the size ratio was fixed at 3.2. Qualitatively, the data seems to be divided into two distinct regions. For particle shapes with aspect ratio below 1, the avalanche size is lower compared to the particle shapes with aspect ratio above 1. No specific trend, however, is observed within these individual regions. The explanation for the observed behavior in that case will be more generic and applicable for aspect ratio values below or above threshold, i.e. 1.0 in this case. As can be seen from fig. 3, the particle shapes with aspect ratio value below 1 are more flatter while those having aspect ratio value above 1 are more elongated in shape. We conjecture better packing of flatter particles with the voids plugged by the secondary spheres resulting in a better packing, lower kinetic energy, higher probability of clogging and thereby reduced avalanche size. On the other hand, the packing may not be efficient in case of elongated particles leaving a lot of void space, which is not possible to be filled in by the number of spheres. This results in lesser packed structure, reduced tendency to clog, hence larger avalanche size.

4 Conclusion

We have studied of flow and clogging behavior of aspherical shaped particles in a silo in presence of secondary spherical particles. All the work was carried out using discrete element method (DEM) simulations for a fixed width of exit orifice and the behavior was primarily accounted in terms of the avalanche size of particles. The overall observations suggest that the probability of clogging is governed by the ability of the primary aspherical particles to pack in presence of secondary spheres. This packing ability was investigated for a wide range of different parameters, viz. sphere volume fraction, particle size ratio, particle shape and silo fill height. In all the cases, it was observed that the probability of clogging can be attributed to two dominant effects, viz. increase in total fraction due to filling up of voids by secondary spheres conducive to clogging and reduced mean particle size exiting the silo which acts against the clogging tendency. It is expected that the results of this work would be of interest to various industrial processes handling powder material, which may contain trace amount of impurities leading to unexpected issues in their flowability.

Acknowledgements

The authors are grateful to Dr. Pankaj Doshi for several fruitful discussions and insightful suggestions. The authors gratefully acknowledge the financial support from Science & Engineering Research Board, India (Grant No. CRG/2019/000423) and “PARAM Brahma Facility” at the IISER, Pune and the “Einstein cluster facility” at CSIR - National Chemical Laboratory Pune.

References

- [1] I. Zuriguel, D.R. Parisi, R.C. Hidalgo, C. Lozano, A. Janda, P.A. Gago, J.P. Peralta, L.M. Ferrer, L.A. Pugnali, E. Clément et al., Clogging transition of many-particle systems flowing through bottlenecks, *Sci. Rep.* **4**, 7324 (2014).
- [2] I. Zuriguel, A. Janda, R. Arévalo, D. Maza, A. Garcimartín, Clogging and unclogging of many-particle systems passing through a bottleneck, *EPJ Web. Conf.* **140**, 01002 (2017).
- [3] R.C. Hidalgo, A.G. ni Arana, A. Hernández-Puerta, I. Pagonabarraga, Flow of colloidal suspensions through small orifices, *Phys. Rev. E* **97**, 012611 (2018).
- [4] A. Janda, D. Maza, A. Garcimartín, E. Kolb, J. Lanuze, E. Clément, Unjamming a granular hopper by vibration, *Eur. Phys. Lett.* **87**, 24002 (2009).
- [5] A. Kunte, P. Doshi, A.V. Orpe, Spontaneous jamming and unjamming in a hopper with multiple exit orifices, *Phys. Rev. E (Rapid Comm.)* **90**, 020201(R) (2014).
- [6] A.V. Orpe, P. Doshi, Friction-mediated flow and jamming in a two-dimensional silo with two exit orifices, *Phys. Rev. E* **100**, 012901 (2019).
- [7] I. Zuriguel, A. Janda, A. Garcimartín, C. Lozano, R. Arévalo, D. Maza, Silo clogging reduction by the presence of an obstacle, *Phys. Rev. Lett.* **107**, 278001 (2011).
- [8] A. Nicolas, M.N. Kuperman, S. Bouzat, A counterintuitive way to speed up pedestrian and granular bottleneck flows prone to clogging: can 'more' escape faster, *J. Stat. Mech.* p. 083403 (2018).
- [9] M.A. Madrid, C.M. Carlevaro, L.A. Pugnali, M. Kuperman, S. Bouzat, Enhancement of the flow of vibrated grains through narrow apertures by addition of small particles, *Phys. Rev. E* **103**, L030901 (2021).
- [10] S.C. Bhure, P. Doshi, A.V. Orpe, Flow and clogging behavior of a mixture of particles in a silo, *Physics of Fluids* **36**, 053326 (2024).